

## Accepted Manuscript

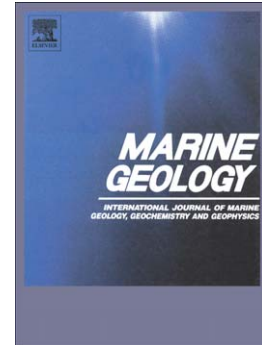
Classifying seabed sediment type using simulated tidal-induced bed shear stress

Sophie L. Ward, Simon P. Neill, Katrien J.J. Van Landeghem, James D. Scourse

PII: S0025-3227(15)00120-6  
DOI: doi: [10.1016/j.margeo.2015.05.010](https://doi.org/10.1016/j.margeo.2015.05.010)  
Reference: MARGO 5302

To appear in: *Marine Geology*

Received date: 19 November 2014  
Revised date: 22 May 2015  
Accepted date: 26 May 2015



Please cite this article as: Ward, Sophie L., Neill, Simon P., Van Landeghem, Katrien J.J., Scourse, James D., Classifying seabed sediment type using simulated tidal-induced bed shear stress, *Marine Geology* (2015), doi: [10.1016/j.margeo.2015.05.010](https://doi.org/10.1016/j.margeo.2015.05.010)

This is a PDF file of an unedited manuscript that has been accepted for publication. As a service to our customers we are providing this early version of the manuscript. The manuscript will undergo copyediting, typesetting, and review of the resulting proof before it is published in its final form. Please note that during the production process errors may be discovered which could affect the content, and all legal disclaimers that apply to the journal pertain.

## Classifying seabed sediment type using simulated tidal-induced bed shear stress

Sophie L. Ward<sup>a,\*</sup>, Simon P. Neill<sup>a</sup>, Katrien J.J. Van Landeghem<sup>a</sup>, James D. Scourse<sup>a</sup>

<sup>a</sup>*School Of Ocean Sciences, Bangor University, Menai Bridge, Isle of Anglesey, LL59 5AB, UK*

---

**Abstract**

An ability to estimate the large-scale spatial variability of seabed sediment type in the absence of extensive observational data is valuable for many applications. In some physical (e.g. morphodynamic) models, knowledge of seabed sediment type is important for inputting spatially-varying bed roughness, and in biological studies, an ability to estimate the distribution of seabed sediment benefits habitat mapping (e.g. scallop dredging). Although shelf sea sediment motion is complex, driven by a combination of tidal currents, waves, and wind-driven currents, in many tidally energetic seas, such as the Irish Sea, long-term seabed sediment transport is dominated by tidal currents. We compare observations of seabed sediment grain size from 242 Irish Sea seabed samples with simulated tidal-induced bed shear stress from a three-dimensional tidal model (ROMS) to quantitatively define the relationship between observed grain size and simulated bed shear stress. With focus on the median grain size of well-sorted seabed sediment samples, we present predictive maps of the distribution of seabed sediment classes in the Irish Sea, ranging from mud to gravel. When compared with the distribution of well-sorted sediment classifications (mud, sand and gravel) from the British Geological Survey digital seabed sediment map of Irish Sea sediments

---

\*Corresponding Author: Sophie L. Ward; Email: [sophie.ward@bangor.ac.uk](mailto:sophie.ward@bangor.ac.uk); Phone: +44 (0)1248 38 39 78

(DigSBS250), this ‘grain size tidal current proxy’ (GSTCP) correctly estimates the

observed seabed sediment classification in over 73% of the area.

*Keywords:* Seabed sediments, Sediment transport, Tidal modelling, Bed shear

stress, ROMS, Irish Sea

---

## 1 **1. Introduction**

2       The large-scale redistribution of sediments in shelf sea regions by  
3 hydrodynamical processes has direct implications for geological basin and coastal  
4 evolution. Seabed sediments also determine the turbidity of water, provide a  
5 substrate for marine benthic organisms, host organic matter and are involved in  
6 biogeochemical exchanges. Shelf sea sediment motion under the influence of tides,  
7 waves and wind-driven currents is a complex phenomenon, the relative contributions  
8 of which can change on complex spatial and temporal scales (van der Molen, 2002;  
9 Porter-Smith et al., 2004; Neill et al., 2010).

10       In a tide-dominated shelf sea such as the Irish Sea, sediment transport in the  
11 nearshore (coastal) zone can be dominated by wave action, whereas farther offshore  
12 the characteristics of seabed sediment distribution are more indicative of the tidal  
13 current conditions of a region (e.g. van Dijk and Kleinhans, 2005; Van Landeghem  
14 et al., 2009b). A number of studies have used the distribution of peak bed shear  
15 stress vectors from tidal models to infer sediment transport pathways and the  
16 location of bedload partings around the British Isles (Pingree and Griffiths, 1979;  
17 Austin, 1991; Harris and Collins, 1991; Aldridge, 1997; Hall and Davies, 2004; Neill  
18 and Scourse, 2009) as well as for the evolution of bathymetric features such as tidal  
19 sand ridges (e.g. Huthnance, 1982; Hulscher et al., 1993), in particular in the Celtic  
20 and Irish Seas (e.g. Belderson et al., 1986; Scourse et al., 2009; Van Landeghem

21 et al., 2009a). Pingree and Griffiths (1979) were the first to model the correlation  
22 between sand transport paths and the peak bed shear stress vectors caused by the  
23 combined  $M_2 + M_4$  tidal currents for many areas on the UK shelf. They found that  
24 the direction of bedload transport correlates with the peak bottom bed shear stress  
25 vectors ( $M_2 + M_4$ ), and most sand transport occurs in response to the peak current  
26 speed over a tidal cycle.

27 Although the relationship between near-bed hydrodynamics and seabed  
28 sediment textures in tidally-dominated areas have been examined (e.g. Uncles, 1983;  
29 Knebel and Poppe, 2000; Signell et al., 2000), there remains a need to define and  
30 quantify a relationship between a range of simulated current speeds (or bed shear  
31 stresses) and a range of seabed sediment types applicable at regional scales. Such a  
32 relationship would be valuable for several applications, such as informing expensive  
33 field campaigns, or spatial scales for sampling, for incorporating spatially varying  
34 drag coefficients into hydrodynamic models, and for habitat mapping (e.g. for  
35 scallop dredging) (Robinson et al., 2011).

36 The aim of this study is to quantify the relationship between simulated  
37 (numerically modelled) tidal-induced bed shear stress and observed seabed sediment  
38 grain size distribution in the Irish Sea. This relationship is used to develop a proxy,  
39 which we refer to hereafter as the ‘grain size tidal current proxy’ (GSTCP), for  
40 predicting large-scale distribution in seabed sediment type in the Irish Sea. The  
41 study region is introduced in Section 2. In Section 3, the tidal model is described,  
42 and the seabed sediment data are presented in Section 3.2, along with a description  
43 of the sub-selection of the observational data (Section 3.3). A first-order  
44 approximation of the relationship between the simulated bed shear stress and

45 observed seabed sediment grain size is presented in detail in Section 4. The  
 46 applications and limitations of this proxy are discussed in Section 5.

### 47 1.1. Sediment transport theory

48 The effects of currents, waves or by combined current and wave motion on  
 49 sediment dynamics take place primarily through the friction exerted on the seabed.  
 50 This frictional force is referred to as the bed shear stress ( $\tau_0$ ) and is expressed as the  
 51 force exerted by the flow per unit area of bed in terms of the density of water ( $\rho$ )  
 52 and the frictional velocity ( $u_*$ ) such that:

$$\tau_0 = \rho u_*^2 \quad (1)$$

53 Sediment transport (of non-cohesive sediments) occurs when the bed shear stress  
 54 exceeds the threshold of motion,  $\tau_{cr}$ , or threshold Shields parameter ( $\theta_{cr}$ ) (Shields,  
 55 1936), which is a dimensionless form of the bed shear stress and is dependent upon  
 56 the median grain size,  $d_{50}$ :

$$\theta_{cr} = \frac{\tau_{cr}}{g(\rho_s - \rho)d_{50}} \quad (2)$$

57 where  $g$  is the gravitational acceleration and  $\rho_s$  is the grain density. The threshold  
 58 Shields parameter can be plotted against the dimensionless grain size,  $D_*$ , to  
 59 produce the well-known Shields curve (Shields, 1936), which describes the threshold  
 60 of motion beneath waves and/or currents. The dimensionless grain size is given by:

$$D_* = \left[ \frac{g(s-1)^{1/3}}{\nu^2} \right] d_{50} \quad (3)$$

61 where  $\nu$  is the kinematic viscosity of water and  $s$  is the ratio of grain to water  
62 density.

63 Sediment transport occurs through bedload and suspended load transport, and  
64 varies depending on the forcing mechanism e.g. whether it is wave-, current- or  
65 wind-induced motion, or a combination of mechanisms inducing the motion.  
66 Numerous empirically-derived sediment transport formulae are available for  
67 total-load sediment transport by currents (e.g. Engelund and Hansen, 1972; van  
68 Rijn, 1984a,b,c), waves (e.g. Bailard, 1981) and combined currents and waves (e.g.  
69 Bailard, 1981; Soulsby, 1997) in the marine environment. However, these equations  
70 have inherent limitations, such as restrictions on applicable water depths, or ranges  
71 of grain sizes, and as such are inappropriate for application to regional scales, such  
72 as the Irish Sea. Many numerical modelling studies (e.g. Pingree and Griffiths, 1979;  
73 Harris and Collins, 1991; Aldridge, 1997; van der Molen, 2002; van der Molen et al.,  
74 2004; Griffin et al., 2008; Warner et al., 2008b, 2010) and combined modelling and  
75 observational studies (e.g. Harris and Wiberg, 1997; Wiberg et al., 2002) have been  
76 conducted in attempts to understand the role of tides and waves on sediment  
77 transport in coastal regions. This is the first study aimed at generating maps of  
78 estimated sediment grain size distribution on regional scales using both observations  
79 and numerical modelling techniques.

## 80 **2. Case study: Irish Sea**

81 It has long been realised that higher-than-average intensity of energy  
82 dissipation occurs in the shallow shelf seas around the UK (Flather, 1976; Simpson  
83 and Bowers, 1981), with approximately 5 to 6% of the total global tidal dissipation

84 occurring in the Northwest European shelf seas, making it the second most  
85 energetic shelf in the world, second only to Hudson Bay (Egbert and Ray, 2001;  
86 Egbert, 2004). The Irish Sea (Fig. 1), positioned centrally within the Northwest  
87 European shelf seas, is a semi-enclosed body of water, with water depths generally  
88 <150 m, and with a north-south trending 250 m deep channel to the northwest of  
89 the Isle of Man, between Scotland and Ireland. The tides in the Irish Sea are  
90 semi-diurnal (Pingree and Griffiths, 1978), and are dominated by the  $M_2$  and  $S_2$   
91 tidal constituents. Some of the tidal wave, which propagates from the North  
92 Atlantic onto the Northwest European shelf, enters the North Sea (from the north)  
93 and through the English Channel from the southwest, while some energy passes into  
94 the Irish Sea, most of which propagates south to north (Pugh, 1987). The tidal  
95 range in the Severn Estuary (in the Bristol Channel) reaches a maximum of  $\sim 12$  m,  
96 the second largest in the world after the Bay of Fundy.

97 The tidally-dominated Irish Sea is an ideal case study for comparison of  
98 observed grain sizes and simulated bed shear stresses given the abundance of  
99 existing research and information on the composition of the seabed sediment  
100 distribution (e.g. Wilson et al., 2001; Holmes and Tappin, 2005; Blyth-Skyrme  
101 et al., 2008; Robinson et al., 2009; Van Landeghem et al., 2009a), as well as  
102 extensive surveys by the British Geological Survey (BGS). Irish Sea sediments  
103 represent redistributed glacial (or glaciofluvial) materials characterised by a wide  
104 range of grain sizes which have the potential to be fractionated by bed shear stress.  
105 There is a significant diversity of seabed sediment classifications within the Irish Sea  
106 (Fig. 2), including areas of exposed bedrock (mostly limited to the northwest of  
107 Anglesey) and patches of semi-consolidated Pleistocene deposits, both covered in

108 places only by thin transient patches of unconsolidated sediment. The majority of  
109 the seabed consists of sands and gravels, consisting of largely reworked glacial  
110 sediments. In the southern Irish Sea, sandy gravel is the predominant sediment  
111 type. Coarse sediments of glacial and glaciofluvial origin occupy both Cardigan Bay  
112 and St George's Channel. In St George's Channel there are several areas of exposed  
113 till, covered only by thin transitory sediment. Along the coast of Cardigan Bay is a  
114 belt of (mainly) sand which is increasingly muddy towards the mouths of rivers. In  
115 the northern Irish Sea there is a band of gravelly sediment, lying to the south and  
116 north of the Isle of Man which separates areas of muddy and sandy sediments to the  
117 east and west. West of the Isle of Man is a large area of mud, known as the Western  
118 Irish Sea Mud Belt, almost entirely surrounded by sandy mud, which itself is  
119 surrounded by muddy sand. The muddy sediments in the Irish Sea are largely  
120 confined to the Western Irish Sea Mud Belt to the east of the Isle of Man, and to  
121 the Celtic Deep (in the central Celtic Sea) (e.g. Jackson et al., 1995).

122 The UK seabed sediments have been mapped and made available by the BGS  
123 as a 1:250,000 scale (~1.1 km grid spacing) digital map product called DigSBS250,  
124 and this map product includes most of the Irish Sea (Fig. 2). The map is based on  
125 an extensive seabed sample database from grabs of the top 0.1 m, combined with  
126 core and dredge samples. For sediment classification, the standard Folk triangle was  
127 used, based on the percentage gravel and the sand:mud ratio (Folk, 1954). In the  
128 Irish Sea, sediment distribution by classification is typically patchy, with isolated  
129 areas of one sediment type (ranging in size from a few metres to many kilometres)  
130 surrounded by another sediment type in some places, and with irregular boundaries  
131 between categories.



### 3. Methods

#### 3.1. Tidal Model

Tidal currents in the Irish Sea were simulated using the three-dimensional Regional Ocean Modeling System (ROMS) (Shchepetkin and McWilliams, 2005), an open-source, free-surface, terrain-following, primitive equations model. The finite-difference approximations of the Reynolds-averaged Navier-Stokes equations are implemented using the hydrostatic and Boussinesq assumptions. The numerical algorithms of ROMS are described in Shchepetkin and McWilliams (2005).

The domain extent for the Irish Sea tidal model was  $8^{\circ}\text{W}$  to  $2.7^{\circ}\text{W}$  and  $50^{\circ}\text{N}$  to  $56^{\circ}\text{N}$  at a resolution of approximately  $1/60^{\circ}$  longitude and with variable latitudinal resolution ( $1/96^{\circ}$  -  $1/105^{\circ}$ , i.e.  $\sim 1.1$  km grid spacing), using a horizontal curvilinear grid. The bathymetry was derived from 120 arcsecond GEBCO (General Bathymetric Chart of the Oceans,  $\sim 1 \times 1$  km resolution), and a minimum water depth of 10 m was applied, which is consistent with other models at this scale and of the region (e.g. Lewis et al., 2014b, 2015). It should be noted that our model application assumes a solid wall along the entire land/sea boundary, and hence alternate wetting and drying of land cells was not included. Given that the model resolution does not fully resolve intertidal regions, the minimum water depth of 10 m, and the lack of wetting and drying, are considered acceptable at this scale.

The model was forced at the boundaries using surface elevation (Chapman boundary conditions) and the  $u$  and  $v$  components of depth-averaged tidal current velocities (Flather boundary conditions), derived from the harmonic constants of the OSU TOPEX/Poseidon Global Inversion Solution 7.2 (TPXO7.2,  $1/4^{\circ}$  resolution globally) (Egbert et al., 1994; Egbert and Erofeeva, 2002). The tidal constituents

156 considered in the derivation of the boundary conditions were  $M_2$  and  $S_2$ . The model  
157 was run for 30 days, from which the last 15 days of model output were analysed.

158 The model was run with analytical expressions for surface momentum stress,  
159 bottom and surface salinity fluxes, bottom and surface temperature flux, free-surface  
160 boundary conditions, and two-dimensional momentum boundary conditions. The  
161 coefficients of vertical harmonic viscosity and diffusion were set to be computed  
162 using the generic lengthscale (GLS) turbulence closure scheme model tuned to  
163  $K - \epsilon$  ( $p=3$ ,  $m=1.5$ , and  $n=-1$ ) (Umlauf and Burchard, 2003; Warner et al., 2005;  
164 Hashemi and Neill, 2014). The tidal model was thus effectively ‘three-dimensional  
165 barotropic’, set to have ten layers in the sigma coordinate, using the coordinate  
166 system of Shchepetkin and McWilliams (2005). As much as was possible without  
167 compromising the accuracy of the model, the resolution of the layers was increased  
168 towards the bed by adjusting the values of the sigma coordinate bottom/surface  
169 control parameters in the model runtime options. The option for quadratic bottom  
170 drag scheme was implemented, using a bottom drag coefficient of 0.003. The  
171 three-dimensional (i.e. depth-varying) bed shear stress is automatically set to be  
172 calculated at the mid-depth of each computational cell, and the model was also set  
173 to compute and output depth-averaged bed shear stress (and tidal current speeds).  
174 So, for example, the ‘near-bed’ shear stress was calculated at the mid-depth of the  
175 lowest vertical layer, the depth of which varied with water depth.

176 The simulated  $M_2$  and  $S_2$  tidal constituents separated using harmonic analysis  
177 (T\_TIDE Pawlowicz et al., 2002) were compared with harmonic constants from six  
178 tide gauges within the UK tide gauge network (National Tidal and Sea Level  
179 Facility, 2012) (Table 1, Fig. 3). The root mean square error (RMSE) was 16 cm in

180 amplitude and  $9^\circ$  in phase ( $M_2$ ), and 5 cm in amplitude and  $8^\circ$  in phase ( $S_2$ ).

Table 1: Observed and simulated amplitudes ( $h$ , in metres) and phases ( $g$ , in degrees relative to Greenwich) of the  $M_2$  and  $S_2$  tidal constituents. The numbers indicate the position of the tide gauges in Figure 3. The Scatter Index is the RMSE normalised by the mean of the data, and given as a percentage.

Tide Gauge	Observed				Modelled			
	$M_2$		$S_2$		$M_2$		$S_2$	
	h	g	h	g	h	g	h	g
Port Erin (1)	1.83	322	0.56	1	1.54	329	0.46	4
Llandudno (2)	2.69	310	0.87	351	2.47	317	0.83	356
Holyhead (3)	1.81	292	0.59	329	1.66	297	0.58	331
Fishguard (4)	1.35	207	0.53	248	1.36	212	0.55	255
Mumbles (5)	3.12	172	1.12	220	3.03	186	1.06	233
Ilfracombe (6)	3.04	162	1.10	209	3.03	174	1.07	221
<b>Scatter Index (%)</b>					<b>6.9</b>	<b>4</b>	<b>6.3</b>	<b>4</b>

181 To validate the tidal current speeds (Fig. 3), published current data from 19  
 182 offshore current meters within the model domain were used (see Jones, 1983; Davies  
 183 and Jones, 1990; Young et al., 2000, for further details). The data were compared  
 184 with the simulated depth-averaged current speed at the grid point nearest the  
 185 offshore current meter location, which was also analysed using T\_TIDE. The  
 186 RMSEs of the  $M_2$  tidal currents were  $5.3 \text{ cm s}^{-1}$  in amplitude and  $12.7^\circ$  in phase,  
 187 and were  $1.9 \text{ cm s}^{-1}$  and  $12.4^\circ$  and  $14.3^\circ$  in phase for the  $S_2$  tidal currents. The  
 188 scatter index is also provided in Fig. 3, which is the RMSE normalised by the mean  
 189 of the data, and given as a percentage. The model was found to perform reasonably

190 well when compared with the performance of other models of the region, which were  
191 of a similar spatial scale (e.g. Neill et al., 2010; Lewis et al., 2015), giving confidence  
192 in the simulated tidal currents.

### 193 *3.2. Seabed sediment data*

194 Data on observed seabed sediments were available from a number of projects,  
195 namely HabMap (Robinson et al., 2011), the South West Irish Sea Survey (SWISS,  
196 Wilson et al., 2001), the Irish Sea Aggregates Initiative (IMAGIN, Kozachenko  
197 et al., 2008), Application of Seabed Acoustic Data in Fish Stocks Assessment and  
198 Fishery Performance (ADFISH, Coastal and Marine Research Centre, 2008), and  
199 data from the Joint Nature and Conservation Committee (JNCC, e.g.,  
200 Blyth-Skyrme et al., 2008). Sediment samples from around the Isle of Man were  
201 collected and analysed as part of work funded by the Isle of Man, Department of  
202 Environment, Food and Agriculture (unpublished data). The full dataset consists of  
203 1105 analysed sediment grab samples, ranging in grain size from mud to boulders.  
204 The samples were analysed using wet sieving and for more detailed analysis of grain  
205 size statistics, the results of the wet sieving were analysed using the GRADISTAT  
206 software (Blott and Pye, 2001). The granulometric analysis used here for calculating  
207 the sample statistics was the graphical method of Folk and Ward (1957).

208 For comparison with model output, the seabed sediment data were sorted by  
209 location and fitted to the computational grid, where each grid cell represented an  
210 area of approximately 1.2 km<sup>2</sup>. Samples taken from locations within the same grid  
211 cell were combined and the mean, minimum, maximum, and a range of grain size  
212 parameters (e.g.  $d_{50}$ ) were calculated for each grid cell containing data (Fig. 4a). To

213 ensure that no nearshore samples were included, and as an approximation of where  
214 nearshore wave effects are likely to dominate sediment transport in this otherwise  
215 tidally-dominated region, all samples from locations with water depths  $\leq 10$  m in  
216 the model bathymetry were removed, which was consistent with the minimum water  
217 depth set in the model bathymetric grid (Section 3.1). This process of gridding the  
218 sediment data, and removing nearshore points resulted in 718 model grid cells  
219 containing data (locations shown in Fig. 4a), reduced from the original 1105  
220 samples.

### 221 3.3. Seabed sediment sorting

222 Determining which grain size parameter correlated best with simulated bed  
223 shear stress was an iterative process. When the median sediment grain size data  
224 from the 718 gridded sediment samples were compared with simulated peak bed  
225 shear stress, there was no discernible correlation (Fig. 4b). Various criteria were  
226 thus investigated and applied to the seabed sediment dataset, including grain size  
227 limits and degree of sediment sorting. The first grain size parameter to be  
228 considered was sorting, since the accuracy of the calculations of median grain size  
229 improved with the degree of sorting of a sample. Sorting is defined within the  
230 GRADISTAT software as the standard deviation (see Blott and Pye, 2001). It is  
231 difficult to calculate  $d_{50}$  for mixed sediment samples, and so the focus of this study  
232 is on the median grain size. Furthermore, the GSTCP is based on a relationship  
233 between sediment classes that have been reworked by tidal currents, and the factors  
234 influencing the spatial distribution of mixed sediment classes is unlikely to be  
235 dominated by tidal currents. All *extremely poorly-sorted*, *very poorly-sorted* and

236 *poorly-sorted* samples were thus removed from the seabed sediment dataset. This  
237 reduced the sample size considerably, from 718 to 273 samples, consisting of only  
238 *moderately-sorted*, *moderately well-sorted*, *well-sorted* and *very well-sorted* samples.

239 Of the 273 *moderately to very well-sorted* samples, 12 had  $d_{50} > 64$  mm (larger  
240 than pebbles), and only 8 had  $d_{50} < 4$   $\mu\text{m}$  (very fine silt). These very fine seabed  
241 sediment samples were taken off the north coast of the Llŷn Peninsula, and to the  
242 northwest of Anglesey. When these very coarse and very fine sediments were  
243 considered, there was no clear positive correlation between grain size and simulated  
244 bed shear stress. These 20 samples were so few (i.e.  $< 10\%$ ) that they were removed  
245 from the dataset, hence the remaining 256 seabed sediment samples were all within  
246 the sand fraction. The removal of these samples was justified as they did not  
247 comprise the mobile fraction, as coarse gravels and cohesive sediments are not  
248 representative of the dynamic equilibrium between tidal current speeds and seabed  
249 sediment type. Fourteen significant outliers remained, which were fine (or very fine)  
250 sands found in areas containing high tidal current speeds (in the Bristol Channel  
251 and off the north coast of Pembrokeshire), where simulated peak bed shear stress  
252 was  $> 10$   $\text{N m}^{-2}$ . These samples were also removed from the seabed sediment  
253 dataset as they were likely to be either cohesive or not in dynamic equilibrium,  
254 leaving 242 gridded seabed sediment sample points. All of the subset of 242 gridded  
255 seabed sediment samples (shown in Fig. 5) were from water depths in the range  
256 10-100 m. Almost half the samples (118 of 242) were from water of 10-15 m depth,  
257 and 216 (of 242) of the samples were taken in water shallower than 50 m.

258 **4. Results**259 *4.1. Grain size tidal current proxy (GSTCP)*

260 The spatial variation in the peak tidal-induced bed shear stress across the Irish  
261 Sea can be seen in Fig 6. There are regions of particularly high bed shear stresses in  
262 the Bristol Channel (where they exceed  $15 \text{ N m}^{-2}$ ), off the Pembrokeshire coast,  
263 northwest of Anglesey, north of the Isle of Man and in the North Channel.

264 Although there is a clearly positive correlation between bed shear stress and seabed  
265 sediment grain size (Fig. 7), the relationship is non-linear in nature, as expected  
266 from the characteristics of the Shields curve (Shields, 1936) which describes the  
267 non-linear variation in the threshold of motion of sediments between currents  
268 (and/or waves), or the Hjulström curve (Hjulstrom, 1935) which describes erosion,  
269 deposition or transport of sediment in rivers (i.e. uni-directional flows).

270 The model outputs of peak bed shear stress were binned into classes of very  
271 low through to high bed shear stress: 0-0.5, 0.5-1, 1-1.5, 1.5-2, 2.5-3, 3-4, 4-5, 5-8  
272 and  $8-10 \text{ N m}^{-2}$ . The observed  $d_{50}$  from model grid cells with bed shear stress  
273 within each class were combined and plotted against the corresponding mid-point of  
274 the bed shear stress range (Fig. 8a). The minimum and maximum of the gridded  
275 median  $d_{50}$  were also noted for each of the bed shear stress ranges and are included  
276 in Fig. 8a.

277 A number of sediment classes from the Wentworth scale (Wentworth, 1922)  
278 were considered, namely very fine sand (and finer,  $<125 \mu\text{m}$ ), fine sand (125-250  
279  $\mu\text{m}$ ), medium sand (250-500  $\mu\text{m}$ ), coarse sand (500-1000  $\mu\text{m}$ ), very coarse sand  
280 (1000-2000  $\mu\text{m}$ ) and gravel ( $>2000 \mu\text{m}$ ). The ranges in simulated bed shear stresses  
281 from locations in which observations of these sediment classes were made were

282 recorded (Fig. 8b). The values used in the GSTCP are given in Table 2. These  
 283 seabed sediment size ranges were then applied to the Irish Sea tidal model output of  
 284 peak bed shear stress, thus demonstrating for the first time a method for predicting  
 285 large-scale patterns in the distribution of sediment classification for specific  
 286 simulated bed shear stress values (Fig. 9a). A version of the DigSBS250 map, which  
 287 only shows selected sediment classes, is provided for comparison (Fig. 9b).

Table 2: Details of the grain size tidal current proxy (GSTCP)

Peak simulated bed shear stress range ( $\text{N m}^{-2}$ )	GSTCP grain size range ( $\mu\text{m}$ )	GSTCP sediment classification
<0.25	<125	very fine sand
0.25 - 0.6	125 - 250	fine sand
0.6 - 3.2	250 - 500	medium sand
3.2 - 4.1	500 - 1000	coarse sand
4.1 - 9	1000 - 2000	very coarse sand
>9	>2000	gravel

#### 288 4.2. Validating the GSTCP

289 The main limitation of the validation of the GSTCP is the practical difficulty  
 290 in acquiring enough seabed sediment grain size data over the shelf. The available  
 291 grain size data have been used in the development of the proxy, and in the absence  
 292 of another extensive dataset, an attempt was made at a more ordinal validation of  
 293 the GSTCP than the qualitative comparison shown in Fig. 9, a significant  
 294 constraint being the difficulty of estimating a median grain size using Folk sediment



295 classifications. Since samples which were classified as mixed (such as muddy gravel)  
296 were eliminated from the sample dataset, a comparison was made between the  
297 mapped areas of mud, sand and gravel only from the DigSBS250 (Fig. 10a) with the  
298 mud, sand and gravel regions estimated by the proxy. For this comparison the  
299 estimated very fine sand (and finer,  $<125\ \mu\text{m}$ ) were classified as mud, fine, medium  
300 and coarse sands were simply classified as sands, and estimated grain sizes  $>2000$   
301  $\mu\text{m}$  were classified as gravel. The spatial differences in observed and estimated areas  
302 of mud, sand and gravel are shown in Fig. 10b. The light grey areas in Fig. 10b  
303 show areas of the seabed where the estimated and observed seabed sediment  
304 classification were in agreement (73% of the non-mixed sediment area). The red and  
305 blue patches indicate where the GSTCP underestimated (15%) and overestimated  
306 (12%) the observed seabed sediment grain size respectively. It should be noted that  
307 the DigSBS250 product is also a generalisation of the Irish Sea seabed sediment  
308 types produced from extensive sediment samples (and hence in many areas is also  
309 estimated and/or interpolated). The differences in the observed and estimated  
310 seabed sediment classification were found to be only between mud and sand, or sand  
311 and gravel, and not between gravel and mud. Although tidal asymmetry is not  
312 accounted for within the GSTCP, there was no correlation between simulated  
313 regions of bed shear stress convergence/divergence and regions of discrepancies  
314 between observed and estimated grain sizes.

## 315 5. Discussion

316 Predicting (albeit large-scale) patterns in seabed sediment type on regional  
317 scales using tidal model output has several key applications, including physical (e.g.

318 morphodynamic) modelling and biological studies, where information regarding the  
319 distribution of seabed sediments is important. For example, the GSTCP could be  
320 used in ecological studies to identify initial areas of interest based on seabed  
321 sediment class, which would then require more focussed investigation (or sampling)  
322 of small-scale variations in substrate type. Knowledge of the physical properties of  
323 an area, including energy regime, topography and substrate type, is essential for  
324 predictive habitat mapping which is used to predict the biological community on the  
325 seabed. A tool for predicting large-scale distributions of seabed sediments is very  
326 valuable, can reduce the need for expensive field campaigns, or can be used to  
327 identify areas of interest for further work. In addition, the GSTCP can be used to  
328 generate predictive maps for seabed sediment evolution over various timescales.  
329 Prior to this work there has been no attempt at generating maps of estimated  
330 sediment grain size distribution on regional scales. Although this proxy is applicable  
331 to high mid-latitude glaciated shelf seas supplied with heterogeneous sediments  
332 available for re-distribution post-glacially, the application of this technique of  
333 estimating grain size distribution on low-latitude shelf seas may be problematic  
334 because of a lack of heterogeneous material available for redistribution.

335 The GSTCP is essentially an attempt at deriving critical threshold values for  
336 sediments in the field which are highly variable in terms of hydrodynamics and  
337 sediment dynamics. Although tidal-induced currents dominate sediment transport  
338 in much of the Irish Sea, other factors such as waves, the influence of which varies  
339 temporally and spatially, play considerable roles in determining sediment dynamics.  
340 Rather than there being a definitive threshold condition to define which current  
341 speeds displace certain grain sizes, a range of threshold values exist (Paphitis, 2001),

342 due to the complexity and stochastic nature of the factors which can influence  
343 sediment transport. This range is not specifically accounted for in the GSTCP,  
344 which further highlights the need to consider the GSTCP as a predictor of  
345 *large-scale* patterns in seabed sediment type. Defining empirical curves for the  
346 threshold of sediment motion (e.g. Hjulstrom, 1935; Shields, 1936; Miller et al.,  
347 1977) is notoriously difficult, as there is considerable scatter in the data (Miller  
348 et al., 1977; Paphitis, 2001). Although these threshold curves are simple to use, they  
349 remain severely restricted by the conditions under which they were developed and,  
350 as such, are not applicable to regional model outputs. The fact that selection  
351 criteria had to be applied to the seabed sediment dataset in order to produce a  
352 discernible trend highlights the limitations of existing theories and empirical  
353 equations for estimating sediment transport.

#### 354 *5.1. Discrepancies between observed and estimated seabed sediment grain sizes*

355 The attempt at quantifying the accuracy of the proxy has inherent limitations.  
356 For example, the Eastern Irish Sea Mud Belt, east of the Isle of Man, is comprised  
357 of fine mixed sediments (such as sandy mud). These fine mixed sediments are  
358 omitted from the comparison and hence the over-estimation of the grain size in this  
359 area (medium sand) is not highlighted in the proxy validation.

360 The proxy did not predict some of the observed isolated patches of gravel, such  
361 as north of Anglesey, and in the North Channel. The main area where the GSTCP  
362 over-estimated the sediment classification was in the area of the Western Irish Sea  
363 Mud Belt. The area of mud in the western Irish Sea corresponds with low tidal  
364 current speeds, suggesting this accumulation is strongly controlled by low

365 hydrodynamic energy. However, other factors, such as mixing (by hydrodynamic  
366 processes or by bioturbation), likely influence this muddy area, since the upper few  
367 metres of seabed sediment appear to date back several thousand years (e.g.  
368 Kershaw, 1986). It is thus not accurate to assume these sediments have  
369 accumulated as a direct result of present-day bed shear stresses only, which could  
370 account for the discrepancy between the estimated and observed seabed sediment in  
371 this area. There is a narrow band of sandy sediment between the English coast and  
372 the Eastern Irish Sea Mud Belt, which has been identified by Pantin (1991) as  
373 having formed at a lower sea level, but remains exposed due to wave action,  
374 preventing later deposition. The grain size in the area of the mud belt east of the  
375 Isle of Man is over-estimated by the GSTCP, and is defined as fine sand.

376 The observed seabed sediment south of Ireland is coarser than the very fine  
377 sand (and finer) estimated by the GSTCP, as indicated by the red patch south of  
378 Ireland in Fig. 10b, and hence confidence in the results of the GSTCP for this area  
379 is low. It is likely that the coarser sediment body in this region is inherited from  
380 previous (higher bed shear stress) regimes, and is effectively moribund, since the  
381 present-day tidal bed shear stress is too low to entrain the coarse sediments. For  
382 example, Neill et al. (2010) found that there was significant enhancement of bed  
383 shear stress in the Celtic Sea during deglaciation owing to the magnitude of  
384 wave-induced bed shear stress in this region as the shelf was flooded with increasing  
385 sea levels. The linear tidal sand ridges of the Celtic Sea are also considered not to  
386 be in equilibrium with present-day tidal currents but rather moribund relics of a  
387 previously more energetic hydrodynamic regime (Belderson et al., 1986; Uehara  
388 et al., 2006; Scourse et al., 2009). This supports the hypothesis that the coarser

389 sediment distribution in the Celtic Sea is inherited from earlier hydrodynamic  
390 regimes. Further, the observed grain sizes north of Ireland (northwest of the North  
391 Channel) are coarser than estimated by the proxy which could be attributable to  
392 this region of the shelf being more exposed to wind effects. Where areas of the shelf  
393 are exposed to wind (swell) propagating onto the shelf from the Atlantic there is  
394 potential for the wave-induced bed shear stress of these longer-period swell waves to  
395 penetrate to the seabed (Neill et al., 2010), thus affecting sediment transport.  
396 Cardigan Bay (west coast of mid-Wales) is also dominated by wave action (Neill  
397 et al., 2010) and the GSTCP was found to underestimate the grain size throughout  
398 this region.

#### 399 *5.2. Limitations of the GSTCP*

400 The GSTCP is developed using only unimodal sediment classes due to the  
401 difficulty of calculating a median grain size for mixed sediment classifications. The  
402 assumption here is that the distribution of such sediment types will reflect a degree  
403 of sorting by tidal currents and hence be indicative of a dynamic equilibrium  
404 between tidal-induced bed shear stress and seabed sediment grain size.

405 Consideration of fractional transport of heterogeneous sediments is beyond the  
406 scope of this study.

407 The grain size tidal current proxy (GSTCP) is based on several key  
408 assumptions, including assuming tidal current-induced sediment transport only  
409 since wave action (which is particularly high during storm events), and wave-current  
410 interactions, are not accounted for. Further, other sediment transport mechanisms  
411 including fluvial processes, wind drift, storm-surge currents, biological mechanisms,

412 gravitational currents and eddy-diffusive transport of suspended sediment are not  
413 considered. Waves can have a significant contribution to sediment dynamics in shelf  
414 sea regions (e.g. van der Molen, 2002; Wiberg et al., 2002) by inducing a stirring  
415 mechanism into the hydrodynamic system, thus keeping the sediment suspended  
416 and susceptible to net transport by tidal currents. Waves are the primary  
417 mechanism for inter-annual variability in sediment transport due to sensitivity to  
418 variability in atmospheric (wind) forcing (Lewis et al., 2014a). In shallower, inshore  
419 areas of the Irish Sea, nearshore wave effects become more important than  
420 tidal-induced currents for transporting sediments. The minimum water depth of 10  
421 m used in the simulation was considered appropriate for attempting to omit the  
422 influence of such significant nearshore wave action. However, it should be noted that  
423 half of the 242 samples on which the GSTCP is based were taken from water depths  
424 between 10-15 m, and it is likely that waves play a role in the sediment dynamics in  
425 such water depths (van Dijk and Kleinhans, 2005). Since much of the Irish Sea is  
426 sheltered by Ireland from the prevailing swell propagating onto the shelf from the  
427 North Atlantic, this omission of waters less than 10 m deep is considered reasonable  
428 in this first attempt at defining the relationship between simulated tidal-induced  
429 bed shear stress and observed seabed sediment grain size.

430 The Irish Sea is an interesting region in terms of tidal dynamics due to the  
431 tides entering this semi-enclosed water body concurrently from the north and the  
432 south. The complex features of the overall circulation of the region clearly add  
433 complexity to quantifying the relationship between simulated (tidal) bed shear  
434 stress and seabed sediment grain sizes. Although the model outputs considered are  
435 the peak tidal currents (and hence bed shear stresses) identified during a

436 spring-neap cycle, in reality strong mean currents in varying directions might  
437 produce little or zero net sediment transport.

438 At no point are the sediment sources in the Irish Sea identified or considered, a  
439 potential source of error when comparing the output of the GSTCP with the  
440 DigSBS250 map. Winnowing and sediment sorting could, for example, leave behind  
441 as lag, coarser sediments in tidally quiescent areas and hence the GSTCP would  
442 underestimate the grain size in such regions (Harris and Wiberg, 2002). These  
443 samples tend to be poorly-sorted and are likely to be of glacial origin. Consideration  
444 of sediment origin, or present-day sources is outside of the scope of this study.  
445 Further, the GSTCP does not resolve mixed sediment classifications, or cohesive  
446 sediments, which would require alternative sediment transport calculations. The  
447 large areas of white (i.e. mixed sediments) in Fig. 10a highlight the need to conduct  
448 research on mixed sediment types, as this omission is a significant limitation.

449 The tidal model used here assumes a constant drag coefficient (0.003) and does  
450 not take into account spatially-varying seabed texture, grain roughness or bedforms  
451 (e.g. upstanding rock outcrops in mud belts). In the majority of regional-scale  
452 hydrodynamic model studies, spatially-varying bed roughness is not accounted for  
453 since extensive observational data regarding seabed sediment type are required for  
454 the model set-up. The bottom drag in tidal models is usually described using linear  
455 or quadratic friction laws, often using a constant drag coefficient (Pingree and  
456 Griffiths, 1979; van der Molen et al., 2004; Uehara et al., 2006; Neill et al., 2010;  
457 Davies et al., 2011). In models which incorporate varying bed roughness, using  
458 model output of bed shear stress to estimate seabed sediment type is another  
459 iterative problem since varying bottom roughness due to variations in grain size can

460 feed back on tidal energetics, such as bed shear stress and dissipation (Aldridge and  
461 Davies, 1993; Nicolle and Karpytchev, 2007; Kagan et al., 2012). The ability to  
462 calculate variable drag coefficients is dependent upon varying the bottom roughness,  
463 which is defined as a function of median grain size (e.g Li and Amos, 2001; Warner  
464 et al., 2005, 2008b). Of more significance, in terms of bed roughness, are larger-scale  
465 modulations in bottom roughness such as dunes and ripples (Van Landeghem et al.,  
466 2009a; Kagan et al., 2012; Van Landeghem et al., 2012). In the past, inputting the  
467 bottom roughness for calculating varying drag coefficients has been dependent upon  
468 observational seabed sediment data (e.g. Warner et al., 2008a; Wu et al., 2011) or  
469 on roughness lengths estimated by model (morphodynamic) subroutines (Li and  
470 Amos, 2001). Further, where comprehensive regional seabed sediment maps exist, it  
471 is possible to input variable bed roughness into tidal models (e.g. Nicolle and  
472 Karpytchev, 2007), although in this case the issue of estimating a median grain size  
473 of a mixed sediment class remains. This GSTCP addresses the constraints of the  
474 above factors by facilitating an estimation of large-scale (spatial) variations in  
475 median grain size on a regional scale. Altering bed roughness in tidal models can  
476 have important consequences for flows and associated sediment transport (McCann  
477 et al., 2011). For example, increased frictional effects due to increased bed  
478 roughness would decrease tidal current velocities and hence affect residual flows.  
479 This would have an amplified effect on bed shear stress through the altered drag  
480 coefficients and the effect on the current speed.

481 Despite the limitations of the GSTCP, it is able to define and differentiate  
482 between the dominant sediment classifications (mud, sand and gravel) in the Irish  
483 Sea. As a first attempt at generating predictive maps of seabed sediment type on a



484 regional scale, the GSTCP is useful for several applications and can be applied until  
485 further work which includes coupled tide and wave modelling, or which incorporates  
486 mixed sediment types, becomes available.

### 487 *5.3. Recommendations for improving the GSTCP*

488 A higher resolution tidal model (e.g. <100 m grid spacing) would considerably  
489 reduce the need for combining clustered seabed sediment sample data and would  
490 better resolve spatial variations in simulated peak bed shear stress. A higher  
491 resolution model would also resolve the intertidal regions and so implementation of  
492 alternate wetting and drying in the simulations would be important. Coupled tide-  
493 and wave modelling (which can be very expensive) would increase the accuracy of  
494 the proxy by considering wave-induced sediment transport. In the majority of shelf  
495 sea and coastal regions both waves and currents play a role in sediment dynamics;  
496 however, their combined effect is not simply a linear addition of the two  
497 independent effects (e.g. Soulsby, 1997; van der Molen, 2002; Neill et al., 2010)  
498 hence the need for coupled tide- and wave modelling. Furthermore, to resolve the  
499 inter-annual variability in the wave climate, multiple years - or even decades - of  
500 simulations are required (Neill and Hashemi, 2013) which is also very expensive.

501 The GSTCP could be further improved by having more observed seabed  
502 sediment data with better spatial coverage throughout the Irish Sea and from a  
503 greater range of water depths since almost 90% of the samples were taken in water  
504 <50 m deep. The most extensive dataset on Irish Sea seabed sediment types has  
505 been compiled by the BGS and the data collection spanned several decades. The  
506 dataset has been used to generate the digital map product used here (DigSBS250)

507 for comparison with the GSTCP estimations. However, it lacks quantitative data on  
508 sediment grain sizes; rather it focusses on sediment classes. The BGS data are  
509 therefore unsuitable for development of the GSTCP but are an invaluable resource  
510 in validating the accuracy of the sediment distribution estimated by the GSTCP.  
511 The seabed sediment samples used here were readily available and use of many more  
512 samples, with better spatial coverage, would require extensive, expensive, further  
513 sampling campaigns and data analysis. As highlighted by the need to eliminate  
514 mixed sediments from this seabed sediment dataset, quantifying the relationship  
515 between currents and mixed sediment grain sizes is a considerable problem that  
516 requires extensive further work.

## 517 6. Conclusions

518 The proxy for seabed sediment grain size developed here is a first-order  
519 approximation, based on the model output of bed shear stress, using a  $\sim 1.1$  km  
520 model grid resolution and six (reasonably well-sorted) sediment classes. The proxy  
521 (GSTCP) was successful in estimating 73% of the *well-sorted* sediments and in  
522 identifying the main areas of coarse sediments in regions of stronger peak tidal  
523 current speeds (and hence high bed shear stress). Discrepancies between maps of  
524 observed and estimated grain sizes in the Irish Sea are mainly attributed to a lack of  
525 consideration of sediment origin or to wave-induced sediment transport. Despite the  
526 limitations of this proxy, the ability to estimate the grain size distribution of seabed  
527 sediments on shelf seas such as the Northwest European shelf seas has significant  
528 implications for a wide range of applications. Future work should include more  
529 seabed sediment grain size samples, with better coverage across the Irish Sea, and

530 the focus should be on coupled tide- and wave modelling. The proxy could be  
531 applied to simulated bed shear stresses from other tidally-energetic shelf sea regions  
532 and it would be beneficial to develop proxies for shelf seas with contrasting  
533 hydrodynamic regimes. Furthermore, quantification of the relationship between  
534 observed seabed sediment grain size of heterogeneous sediment samples and  
535 simulated bed shear stresses over regional scales would significantly enhance future  
536 similar proxies.

537 **Acknowledgements** Funding was provided by the Natural Environment  
538 Research Council (NERC) through grant NE/I527853/1 (Ph.D. studentship to  
539 SLW). The authors are grateful for access to the seabed sediment sample data and  
540 would like to acknowledge colleagues collecting and preparing these data through  
541 the projects HABMAP, SWISS, IMAGIN, ADFISH, various projects lead by the  
542 JNCC, as well as Hilmar Hinz, Lee Murray and Gwladys Lambert for work  
543 undertaken on a project funded by the Isle of Man Government (Department of  
544 Environment, Food and Agriculture). The author acknowledges modelling support  
545 from Patrick Timko and Reza Hashemi. The digital seabed sediment map  
546 (DigSBS250) was kindly made available by the BGS. The model simulations were  
547 undertaken on High Performance Computing (HPC)Wales, a collaboration between  
548 Welsh universities, the Welsh Government and Fujitsu.

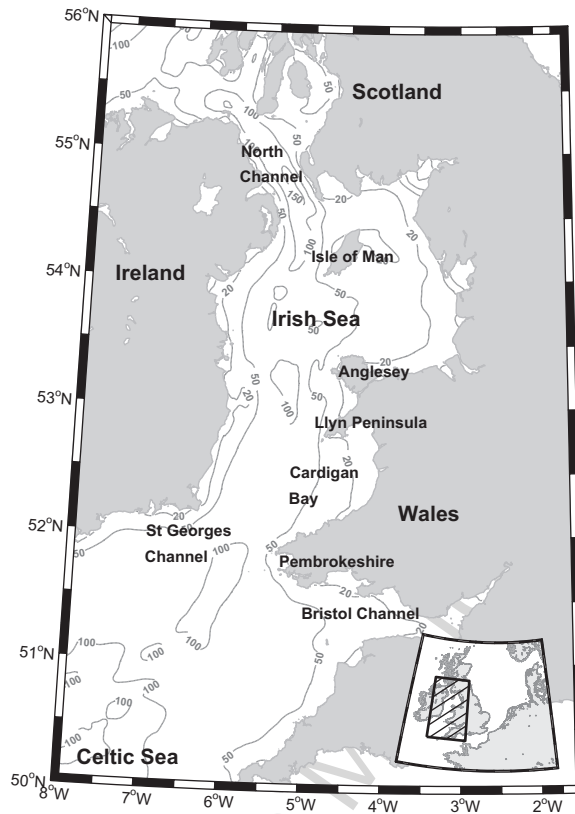


Figure 1: Bathymetry of the Irish Sea, with water depth (mean sea level) contours in metres. Insert map: the position of the Irish Sea on the Northwest European Shelf.

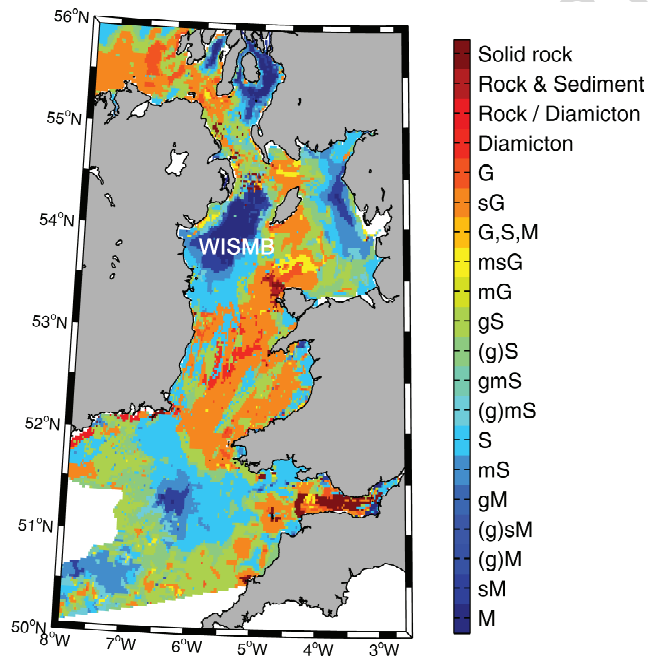


Figure 2: Digital map of the seabed sediment of the UK waters in the Irish Sea, taken from DigSBS250, using the 20 sediment categories defined by Folk (1954). Grey areas are land and white areas indicate where data are not available. The Western Irish Sea Mud Belt (WISMB) has been labelled. Digital map reproduced with permission of British Geological Survey © NERC. All rights reserved.

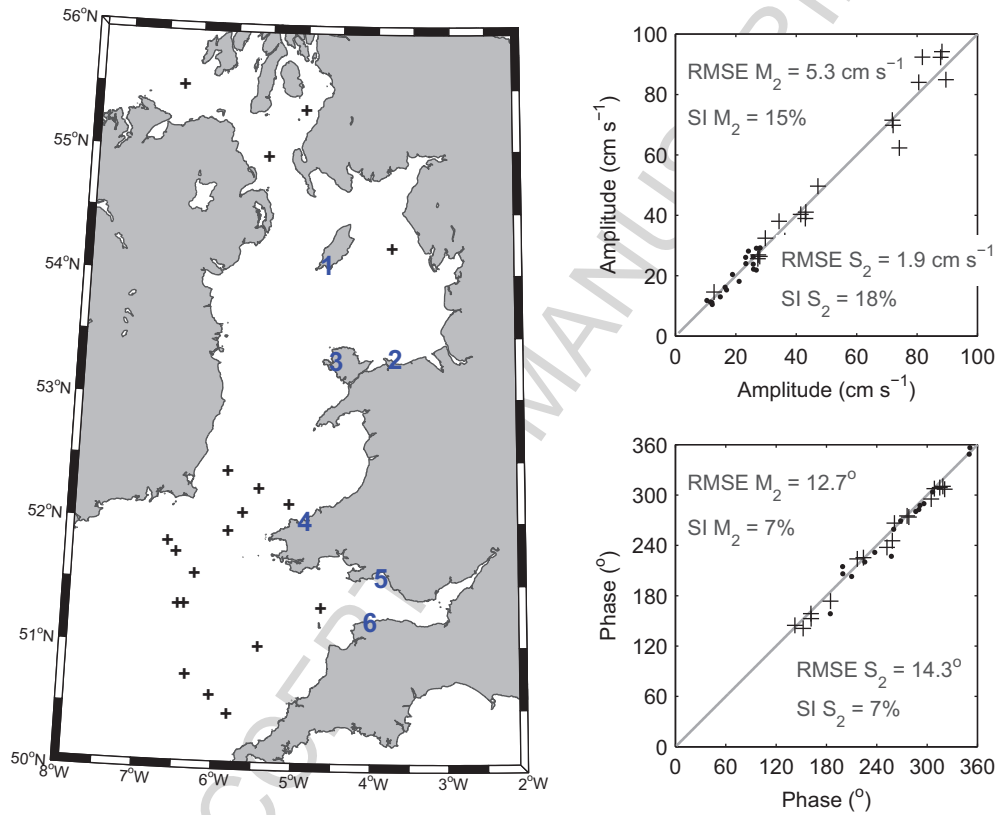


Figure 3: Left panel: The locations of the offshore current meter stations (crosses) and the tide gauge stations (numbers) used in the model validation. Right two panels: Comparison between simulated (x-axis) and observed (y-axis) depth-averaged M<sub>2</sub> (crosses) and S<sub>2</sub> (circles) components of tidal current amplitude (upper panel) and phase (lower panel). RMSE = root mean square error, SI = scatter index.

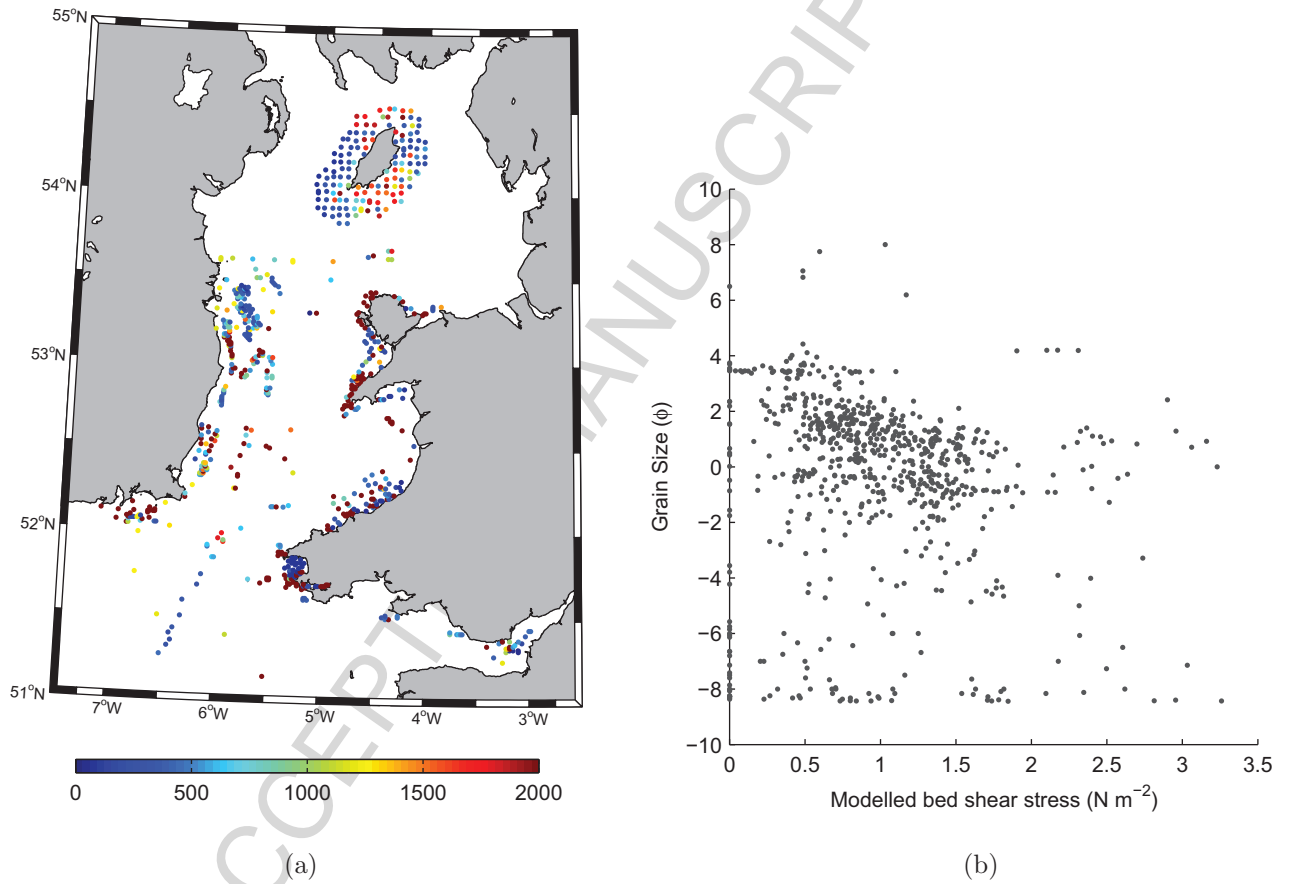


Figure 4: a) Average median grain size,  $d_{50}$  ( $\mu\text{m}$ ), derived from grain size analysis of 1105 seabed sediment samples, which have been combined and gridded into 718 grid cells containing sediment data. b) Correlation between average median grain size,  $d_{50}$  (in  $\phi$  to show the full size range) of all 718 seabed sediment samples and ROMS tidal model output of peak bed shear stress.

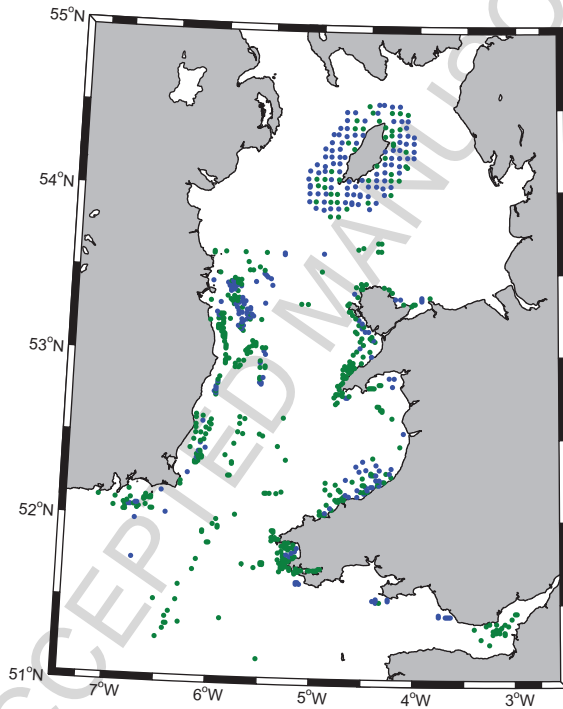


Figure 5: Distribution of gridded seabed sediment samples: blue = 242 samples remaining after application of the various selection criteria, green = 476 samples removed.



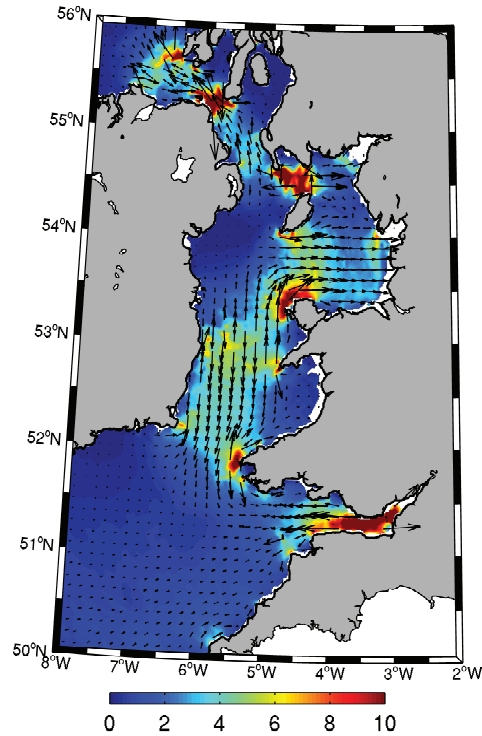


Figure 6: Simulated ‘near-bed’ peak ( $M_2 + S_2$ ) tidal-induced bed shear stress in the Irish Sea (in  $\text{N m}^{-2}$ ). Colour scale denotes the bed shear stress magnitude, and vectors denote the direction and magnitude. White areas show additional land mask or where water depths are  $\leq 10$  m

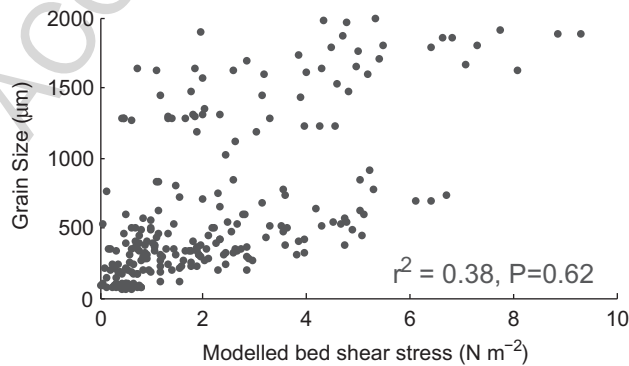


Figure 7: Correlation between gridded seabed sediment samples (mean  $d_{50}$  in  $\mu\text{m}$ ) and ROMS tidal model output of peak bed shear stress. Samples removed from this dataset included those that were less well sorted than *moderately sorted*, very fine samples ( $< 63 \mu\text{m}$ ) in areas of very strong tidal currents, and samples from areas with bed shear stress  $> 10 \text{ N m}^{-2}$ .

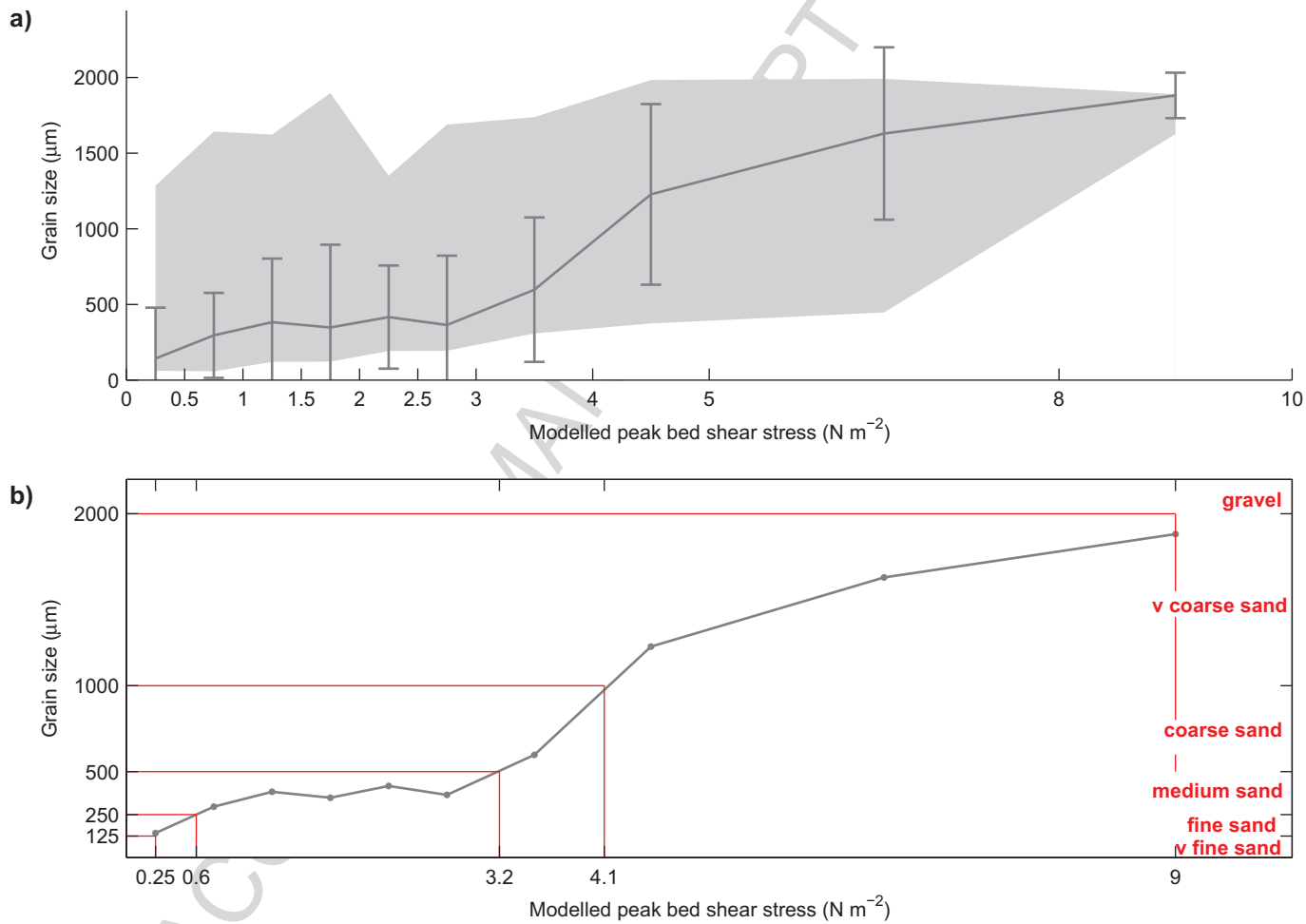


Figure 8: a) Median grain size and associated standard deviations of gridded seabed sediment samples within specified ranges of simulated bed shear stress (grey line), plotted at the mid-point of the bed shear stress classes (x-axis). The range of gridded median grain sizes are also given (grey fill). b) Median grain size of gridded seabed sediment samples (grey line). The red lines relate to the range of bed shear stress (x-axis) for the different sediment classes (y-axis). The sample sorting and grain size selection criteria were applied to these data.

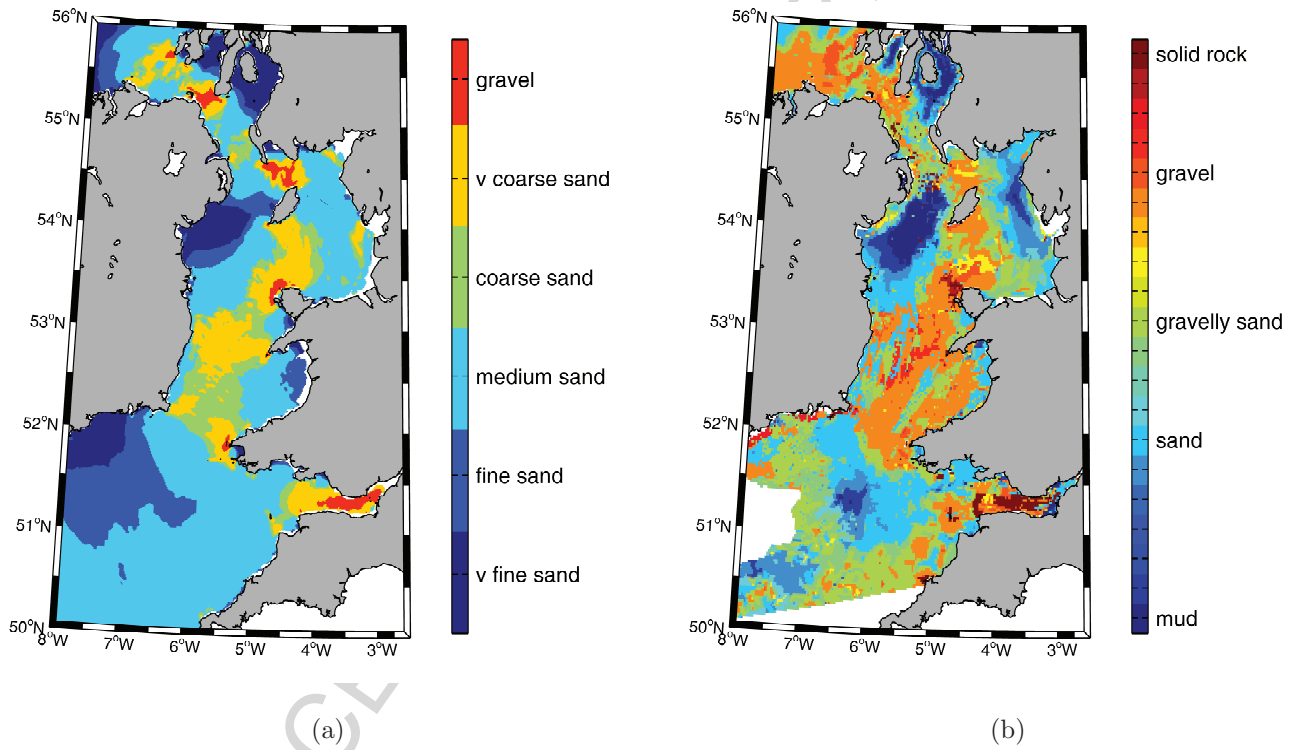


Figure 9: a) Irish Sea seabed sediment distribution estimated by the GSTCP, using simulated bed shear stress. b) Seabed sediments from DigSBS250. Only selected grain size classifications are identified, which indicates a general coarsening of seabed sediment from blue to red on the colour scale.

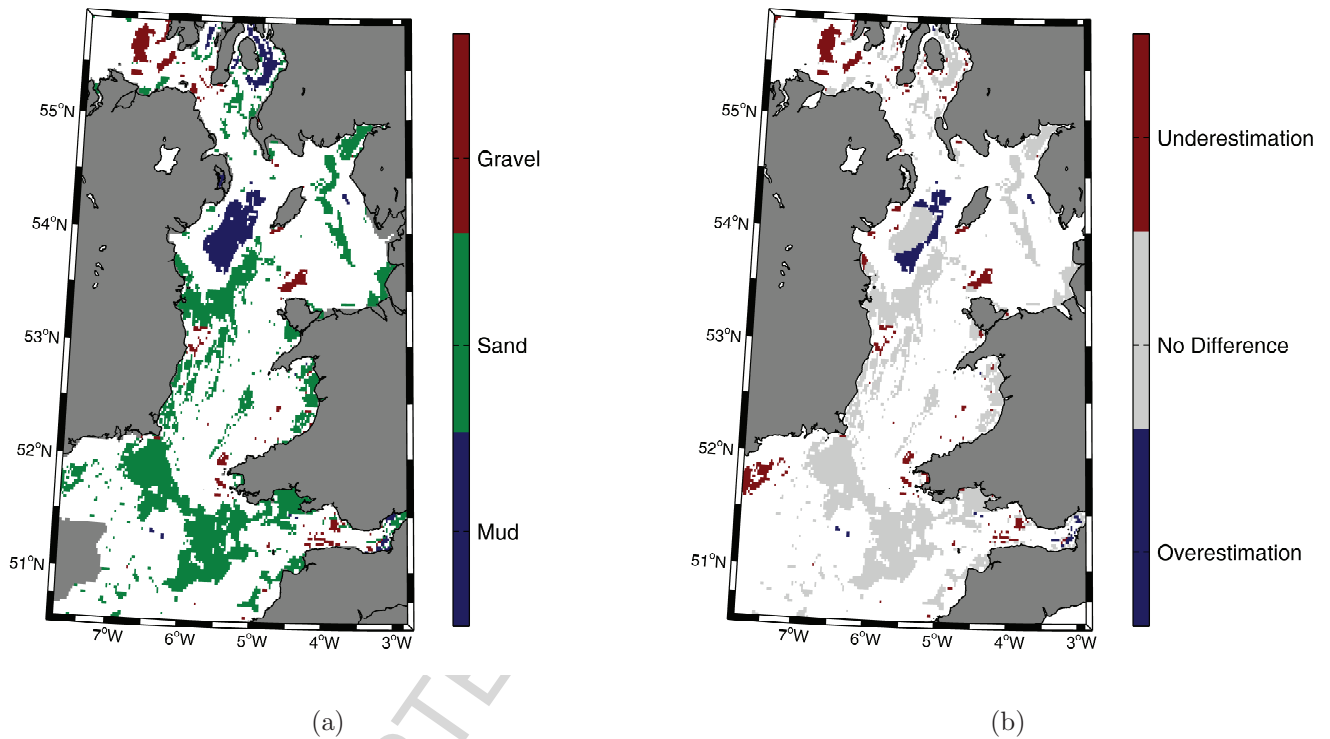


Figure 10: a) Selected seabed sediment classes from DigSBS250 for comparison with the sediment classes estimated by the GSTCP. Only mud (blue), sand (green) and gravel (red) are shown. Mixed sediment classifications are indicated by the white areas. Dark grey areas show land (outlined by the black contour) and where no seabed sediment data were available. b) Difference between the observed and estimated grain size classifications, plotted as the observed minus the estimated. The white areas indicate where seabed sediment was classified as mixed or where there were no seabed sediment data. The light grey areas show areas of agreement between estimated and observed sediment classifications. The red and blue areas indicate where the GSTCP under- and over-estimates the seabed sediment grain size respectively.

549 **References**

- 550 Aldridge, J. N., 1997. Hydrodynamic Model Predictions of Tidal Asymmetry and  
551 Observed Sediment Transport Paths in Morecambe Bay. *Estuarine, Coastal and*  
552 *Shelf Science* 44, 39–56.
- 553 Aldridge, J. N., Davies, A. M., 1993. A High-Resolution Three-Dimensional  
554 Hydrodynamic Tidal Model of the Eastern Irish Sea. *Journal of Physical*  
555 *Oceanography* 23, 207–224.
- 556 Austin, R. M., 1991. Modelling Holocene tides on the NW European continental  
557 shelf. *Terra Nova* 3, 276–288.
- 558 Bailard, J. A., 1981. An energetics total load sediment transport model for a plane  
559 sloping beach. *Journal of Geophysical Research* 86, 10938.
- 560 Belderson, R., Pingree, R., Griffiths, D., 1986. Low sea-level tidal origin of Celtic  
561 Sea sand banks - evidence from numerical modelling of M2 tidal streams. *Marine*  
562 *Geology* 73, 99–108.
- 563 Blott, S. J., Pye, K., 2001. GRADISTAT: a grain size distribution and statistics  
564 package for the analysis of unconsolidated sediments. *Earth Surface Processes and*  
565 *Landforms* 26, 1237–1248.
- 566 Blyth-Skyrme, V., Lindenbaum, C., Verling, E., Van Landeghem, K., Robinson, K.,  
567 Mackie, A., Darbyshire, T., 2008. Broad-scale biotope mapping of potential reefs  
568 in the Irish Sea (north-west of Anglesey). JNCC Report No. 423. Tech. rep.
- 569 Coastal and Marine Research Centre, 2008. ADFISH: Application of Seabed  
570 Acoustic Data in Fish Stocks Assessment & Fishery Performance.  
571 URL  
572 [http://www.cmrc.ie/projects/adfish-application-of-seabed-acoustic](http://www.cmrc.ie/projects/adfish-application-of-seabed-acoustic-data-in-fish-stocks-assessment--fishery-performance.html)  
573 [-data-in-fish-stocks-assessment--fishery-performance.html](http://www.cmrc.ie/projects/adfish-application-of-seabed-acoustic-data-in-fish-stocks-assessment--fishery-performance.html)
- 574 Davies, A. M., Jones, J. E., 1990. Application of a three-dimensional turbulence  
575 energy model to the determination of tidal currents on the northwest European  
576 Shelf. *Journal of Geophysical Research* 95, 18143.
- 577 Davies, A. M., Xing, J., Jones, J. E., 2011. A model study of tidal distributions in  
578 the Celtic and Irish Sea regions determined with finite volume and finite element  
579 models. *Ocean Dynamics* 61, 1645–1667.
- 580 Egbert, G. D., 2004. Numerical modeling of the global semidiurnal tide in the  
581 present day and in the last glacial maximum. *Journal of Geophysical Research*  
582 109, C03003.
- 583 Egbert, G. D., Bennett, A. F., Foreman, M. G. G., 1994. TOPEX/POSEIDON tides  
584 estimated using a global inverse model. *Journal of Geophysical Research* 99,  
585 24821.
- 586 Egbert, G. D., Erofeeva, S. Y., 2002. Efficient Inverse Modeling of Barotropic Ocean  
587 Tides. *Journal of Atmospheric and Oceanic Technology* 19, 183–204.

- 588 Egbert, G. D., Ray, R. D., 2001. Estimates of M2 tidal energy dissipation from  
589 TOPEX/Poseidon altimeter data. *Journal of Geophysical Research* 106, 22475.
- 590 Engelund, F., Hansen, E., 1972. A Monograph on Sediment Transport in Alluvial  
591 Streams, 3rd edn. Technical Press, Copenhagen. Tech. rep.
- 592 Flather, R. A., 1976. A tidal model of the north-west European continental shelf.  
593 *Memoires de la Society Royal des Sciences de Liege* 6 series, 141–164.
- 594 Folk, R., 1954. The distinction between grain size and mineral composition in  
595 sedimentary rock nomenclature. *Journal of Geology* 62, 344–359.
- 596 Folk, R., Ward, W., 1957. Brazos River bar: a study in the significance of grain size  
597 parameters. *Journal of Sedimentary Petrology* 27, 3–26.
- 598 Griffin, J. D., Hemer, M. A., Jones, B. G., 2008. Mobility of sediment grain size  
599 distributions on a wave dominated continental shelf, southeastern Australia.  
600 *Marine Geology* 252, 13–23.
- 601 Hall, P., Davies, A. M., 2004. Modelling tidally induced sediment-transport paths  
602 over the northwest European shelf: the influence of sea-level reduction. *Ocean*  
603 *Dynamics* 54, 126–141.
- 604 Harris, C. K., Wiberg, P., 2002. Across-shelf sediment transport : Interactions  
605 between suspended sediment and bed sediment. *Journal of Geophysical Research*  
606 107.
- 607 Harris, C. K., Wiberg, P. L., 1997. Approaches to quantifying long-term continental  
608 shelf sediment transport with an example from the Northern California STRESS  
609 mid-shelf site. *Continental Shelf Research* 17, 1389–1418.
- 610 Harris, P., Collins, M., 1991. Sand transport in the Bristol Channel: bedload parting  
611 zone or mutually evasive transport pathways? *Marine Geology* 101, 209–216.
- 612 Hashemi, M. R., Neill, S. P., 2014. The role of tides in shelf-scale simulations of the  
613 wave energy resource. *Renewable Energy* 69, 300–310.
- 614 Hjulstrom, F., 1935. Study of the morphological activity of rivers as illustrated by  
615 the Furis. *Bulletin of the Geological Institutions of the University of Uppsala* 25,  
616 221–527.
- 617 Holmes, R., Tappin, D., 2005. DTI Strategic Assessment Area 6, Irish Sea, seabed  
618 and surficial geology and processes. British Geological Survey Commissioned  
619 Report, CR/05/057. Tech. rep.
- 620 Hulscher, S. J., de Swart, H. E., de Vriend, H. J., 1993. The generation of offshore  
621 tidal sand banks and sand waves. *Continental Shelf Research* 13, 1183–1204.
- 622 Huthnance, J. M., 1982. On one mechanism forming linear sand banks. *Estuarine,*  
623 *Coastal and Shelf Science* 14, 79–99.
- 624 Jackson, D. I., Jackson, A. A., Evans, D., Wingfield, R. T. R., Barnes, R. P.,  
625 Arthur, M. J., 1995. The geology of the Irish Sea. (HMSO.). Tech. rep.

- 626 Jones, J., 1983. Charts of O1, K1, N2, M2 and S2 Tides in the Celtic Sea including  
627 M2 and S2 Tidal Currents. Tech. rep.
- 628 Kagan, B. A., Sofina, E. V., Rashidi, E., 2012. The impact of the spatial variability  
629 in bottom roughness on tidal dynamics and energetics, a case study: the M2  
630 surface tide in the North European Basin. *Ocean Dynamics* 62, 1425–1442.
- 631 Kershaw, P., 1986. Radiocarbon dating of Irish Sea sediments. *Estuarine, Coastal  
632 and Shelf Science* 23, 295–303.
- 633 Knebel, H. J., Poppe, L. J., 2000. Seafloor Environments within Long Island Sound:  
634 A Regional Overview. *Journal of Coastal Research* 16, 533–550.
- 635 Kozachenko, M., Fletcher, R., Sutton, G., Monteys, X., Van Landeghem, K.,  
636 Wheeler, A., Lassoued, Y., Cooper, A., Nicoll, C., 2008. A geological appraisal of  
637 marine aggregate resources in the southern Irish Sea. Technical report produced  
638 for the Irish Sea. Technical report produced for the Irish Sea Marine Aggregates  
639 Initiative (IMAGIN) project funded under the INTERREG IIIA Programme.  
640 Tech. rep.
- 641 Lewis, M., Neill, S., Elliott, A. J., 2014a. Inter-annual variability of two contrasting  
642 offshore sand banks in a region of extreme tidal range. *Journal of Coastal  
643 Research* 31, 265–275.
- 644 Lewis, M., Neill, S., Hashemi, M., Reza, M., 2014b. Realistic wave conditions and  
645 their influence on quantifying the tidal stream energy resource. *Applied Energy*  
646 136, 495–508.
- 647 Lewis, M., Neill, S., Robins, P., Hashemi, M., 2015. Resource assessment for future  
648 generations of tidal-stream energy arrays. *Energy* 83, 403–415.
- 649 Li, M. Z., Amos, C. L., 2001. SEDTRANS96: the upgraded and better calibrated  
650 sediment-transport model for continental shelves. *Computers & Geosciences* 27,  
651 619–645.
- 652 McCann, D. L., Davies, A. G., Bennell, J. D., 2011. Bed roughness feedback in  
653 TELEMAC-2D and SISYPHE. In: *Proceedings of the XVIII Telemac and  
654 Mascaret User Club*. pp. 99–104.
- 655 Miller, M. C., McCave, I. N., Komar, P. D., 1977. Threshold of sediment motion  
656 under unidirectional currents. *Sedimentology* 24, 507–527.
- 657 National Tidal and Sea Level Facility, 2012. Real-time data - UK National Tide  
658 Gauge Network.  
659 URL <http://www.ntslf.org/data/uk-network-real-time>
- 660 Neill, S. P., Hashemi, M. R., 2013. Wave power variability over the northwest  
661 European shelf seas. *Applied Energy* 106, 31–46.
- 662 Neill, S. P., Scourse, J. D., 2009. The formation of headland/island sandbanks.  
663 *Continental Shelf Research* 29, 2167–2177.

- 664 Neill, S. P., Scourse, J. D., Uehara, K., 2010. Evolution of bed shear stress  
665 distribution over the northwest European shelf seas during the last 12,000 years.  
666 *Ocean Dynamics* 60, 1139–1156.
- 667 Nicolle, A., Karpytchev, M., 2007. Evidence for spatially variable friction from tidal  
668 amplification and asymmetry in the Pertuis Breton (France). *Continental Shelf*  
669 *Research* 27, 2346–2356.
- 670 Pantin, H. M., 1991. Seabed sediments around the United Kingdom: their  
671 bathymetric and physical environment, grain size, mineral composition and  
672 associated bedforms. Tech. rep., British Geological Survey Marine Geology Series  
673 research report, SB/90/1.
- 674 Paphitis, D., 2001. Sediment movement under unidirectional flows: an assessment of  
675 empirical threshold curves. *Coastal Engineering* 43, 227–245.
- 676 Pawlowicz, R., Beardsley, B., Lentz, S., 2002. Classical tidal harmonic analysis  
677 including error estimates in MATLAB using T\_TIDE. *Computers & Geosciences*  
678 28, 929–937.
- 679 Pingree, R. D., Griffiths, D. K., 1978. Tidal fronts on the shelf seas around the  
680 British Isles. *Journal of Geophysical Research* 83, 4615–4622.
- 681 Pingree, R. D., Griffiths, D. K., 1979. Sand transport paths around the British Isles  
682 resulting from M2 and M4 tidal interactions. *Journal of the Marine Biology*  
683 *Association U.K.* 59, 497–513.
- 684 Porter-Smith, R., Harris, P., Andersen, O., Coleman, R., Greenslade, D., Jenkins,  
685 C., 2004. Classification of the Australian continental shelf based on predicted  
686 sediment threshold exceedance from tidal currents and swell waves. *Marine*  
687 *Geology* 211, 1–20.
- 688 Pugh, D. T., 1987. *Tides, Surges and mean sea-level*. Vol. 5. John Wiley & Sons,  
689 Ltd., Chichester.
- 690 Robinson, K., Darbyshire, T., Van Landeghem, K., Lindenbaum, C., McBreen, F.,  
691 Creavan, S., Ramsay, K., Mackie, A., Mitchell, N., Wheeler, A., Wilson, J.,  
692 O’Beirn, F., 2009. Habitat Mapping for Conservation and Management of the  
693 Southern Irish Sea (HABMAP) I: Seabed Surveys. *Studies in Marine Biodiversity*  
694 *and Systematics from the National Museum of Wales*. Tech. rep.
- 695 Robinson, K., Ramsay, K., Lindenbaum, C., Frost, N., Moore, J., Wright, A.,  
696 Petrey, D., 2011. Predicting the distribution of seabed biotopes in the southern  
697 Irish Sea. *Continental Shelf Research* 31, S120–S131.
- 698 Scourse, J. D., Uehara, K., Wainwright, A., 2009. Celtic Sea linear tidal sand ridges,  
699 the Irish Sea Ice Stream and the Fleuve Manche: Palaeotidal modelling of a  
700 transitional passive margin depositional system. *Marine Geology* 259, 102–111.
- 701 Shchepetkin, A. F., McWilliams, J. C., 2005. The regional oceanic modeling system  
702 (ROMS): a split-explicit, free-surface, topography-following-coordinate oceanic  
703 model. *Ocean Modelling* 9, 347–404.



- 704 Shields, A., 1936. Application of similarity principles and turbulence research to  
705 bedload movement. Tech. rep., Hydrodynamics Laboratory, California Institute of  
706 Technology.
- 707 Signell, R. P., List, J. H., Farris, A. S., 2000. Bottom Currents and Sediment  
708 Transport in Long Island Sound: A Modeling Study. *Journal of Coastal Research*  
709 16, 551–566.
- 710 Simpson, J., Bowers, D., 1981. Models of stratification and frontal movement in shelf  
711 seas. *Deep Sea Research Part A. Oceanographic Research Papers* 28, 727–738.
- 712 Soulsby, R. L., 1997. *Dynamics of Marine Sand*. Thomas Telford, London.
- 713 Uehara, K., Scourse, J. D., Horsburgh, K. J., Lambeck, K., Purcell, A. P., 2006.  
714 Tidal evolution of the northwest European shelf seas from the Last Glacial  
715 Maximum to the present. *Journal of Geophysical Research* 111, C09025.
- 716 Umlauf, L., Burchard, H., 2003. A generic length-scale equation for geophysical  
717 turbulence models. *Journal of Marine Research* 61, 235–265.
- 718 Uncles, R. J., 1983. Modeling Tidal Stress, Circulation, and Mixing in the Bristol  
719 Channel as a Prerequisite for Ecosystem Studies. *Canadian Journal of Fisheries*  
720 and Aquatic Sciences 40, s8–s19.
- 721 van der Molen, J., 2002. The influence of tides, wind and waves on the net sand  
722 transport in the North Sea. *Continental Shelf Research* 22, 2739–2762.
- 723 van der Molen, J., Gerrits, J., de Swart, H., 2004. Modelling the morphodynamics of  
724 a tidal shelf sea. *Continental Shelf Research* 24, 483–507.
- 725 van Dijk, T. A. G. P., Kleinhans, M. G., 2005. Processes controlling the dynamics of  
726 compound sand waves in the North Sea, Netherlands. *Journal of Geophysical*  
727 *Research* 110, F04S10.
- 728 Van Landeghem, K. J., Baas, J. H., Mitchell, N. C., Wilcockson, D., Wheeler, A. J.,  
729 2012. Reversed sediment wave migration in the Irish Sea, NW Europe: A  
730 reappraisal of the validity of geometry-based predictive modelling and  
731 assumptions. *Marine Geology* 295, 95–112.
- 732 Van Landeghem, K. J., Uehara, K., Wheeler, A. J., Mitchell, N. C., Scourse, J. D.,  
733 2009a. Post-glacial sediment dynamics in the Irish Sea and sediment wave  
734 morphology: Data-model comparisons. *Continental Shelf Research* 29, 1723–1736.
- 735 Van Landeghem, K. J., Wheeler, A. J., Mitchell, N. C., Sutton, G., 2009b.  
736 Variations in sediment wave dimensions across the tidally dominated Irish Sea,  
737 NW Europe. *Marine Geology* 263, 108–119.
- 738 van Rijn, L. C., 1984a. Sediment Transport, Part I: Bed Load Transport. *Journal of*  
739 *Hydraulic Engineering* 110, 1431–1456.
- 740 van Rijn, L. C., 1984b. Sediment Transport, Part II: Suspended Load Transport.  
741 *Journal of Hydraulic Engineering* 110, 1613–1641.

- 742 van Rijn, L. C., 1984c. Sediment Transport, Part III: Bed forms and Alluvial  
743 Roughness. *Journal of Hydraulic Engineering* 110, 1733–1754.
- 744 Warner, J. C., Armstrong, B., He, R., Zambon, J. B., 2010. Development of a  
745 Coupled Ocean-Atmosphere-Wave-Sediment Transport (COAWST) Modeling  
746 System. *Ocean Modelling* 35, 230–244.
- 747 Warner, J. C., Butman, B., Dalyander, P. S., 2008a. Storm-driven sediment  
748 transport in Massachusetts Bay. *Continental Shelf Research* 28, 257–282.
- 749 Warner, J. C., Sherwood, C. R., Arango, H. G., Signell, R. P., 2005. Performance of  
750 four turbulence closure models implemented using a generic length scale method.  
751 *Ocean Modelling* 8, 81–113.
- 752 Warner, J. C., Sherwood, C. R., Signell, R. P., Harris, C. K., Arango, H. G., 2008b.  
753 Development of a three-dimensional, regional, coupled wave, current, and  
754 sediment-transport model. *Computers & Geosciences* 34, 1284–1306.
- 755 Wentworth, C. K., 1922. A Scale of Grade and Class Terms for Clastic Sediments.  
756 *The Journal of Geology* 30, 377–392.
- 757 Wiberg, P. L., Drake, D. E., Harris, C. K., Noble, M., 2002. Sediment transport on  
758 the Palos Verdes shelf over seasonal to decadal time scales. *Continental Shelf*  
759 *Research* 22, 987–1004.
- 760 Wilson, J. G., Mackie, A. S. Y., O'Connor, B. D. S., Rees, E. I. S., Darbyshire, T.,  
761 2001. Benthic Biodiversity in the southern Irish Sea 2. The South-West Irish Sea  
762 Survey (SWISS). *Studies in Marine Biodiversity and Systematics from the*  
763 *National Museum of Wales. BIOMÔR Reports* 2(1). Tech. rep.
- 764 Wu, Y., Chaffey, J., Greenberg, D. A., Colbo, K., Smith, P. C., 2011.  
765 Tidally-induced sediment transport patterns in the upper Bay of Fundy: A  
766 numerical study. *Continental Shelf Research* 31, 2041–2053.
- 767 Young, E. F., Aldridge, J. N., Brown, J., 2000. Development and validation of a  
768 three-dimensional curvilinear model for the study of fluxes through the North  
769 Channel of the Irish Sea. *Continental Shelf Research* 20, 997–1035.

### Highlights

- We compare seabed sediment grain size with simulated tidal-induced bed shear stress.
- A proxy for sediment grain size is developed using the quantified relationship.
- Predictive maps of (non-mixed) seabed sediment classes are generated.
- The proxy reproduces large-scale patterns of seabed sediment class distribution.
- Sediment distribution maps are useful in physical modelling and biological studies.